Combined Analysis of Water Stable Isotopes ($H_2{}^{16}O$, $H_2{}^{17}O$, $H_2{}^{18}O$, $HD^{16}O$) in Ice Cores

Amaelle Landais*,**, Eugeni Barkan*, Françoise Vimeux**, Valérie Masson-Delmotte**, Boaz Luz*

* *The Institute of Earth Sciences, The Hebrew University of Jerusalem, Givat Ram, Jerusalem 91904, Israel, amaelle.landais@lsce.ipsl.fr*

** *Institut Pierre Simon Laplace / Laboratoire des Sciences du Climat et de l'Environnement, l'Orme des merisiers, 91191 Gif sur Yvette, France*

Abstract: Water stable isotopes are currently measured in polar ice cores. The long records of $\delta^{18}O$ and δD provide unique information on the past polar temperature while the combination of $\delta^{18}O$ and δD constrains the evolution of the oceanic evaporative regions. Recently, new analytical developments have made it possible to measure with high precision a new isotopic ratio in water, $\delta^{17}O$. As for δD and $\delta^{18}O$, the combination of $\delta^{17}O$ and $\delta^{18}O$ shows a high dependence with the climatic conditions during evaporation. Based on measurements of the different isotopic ratios in Antarctica surface snow, we show that while the combination of $\delta^{18}O$ and δD in the so-called d-excess displays variation with local climatic conditions in the polar regions in addition to the influence of the evaporative regions, the combination of $\delta^{17}O$ and $\delta^{18}O$ in the so-called $^{17}O_{excess}$ is not modified during the air mass transportation above the polar regions. This makes $^{17}O_{excess}$ a simpler parameter than d-excess to constrain the evolution of the oceanic evaporative regions. Finally, records of d-excess and $^{17}O_{excess}$ over the deglaciation in the Vostok ice core suggest significant changes in the evaporative regions. Our interpretation is that the relative humidity over the ocean was higher during the glacial period than today and that reevaporation increased over the deglaciation.

Key words: ice core, water isotopes, water cycle, relative humidity, deglaciation.

1. Introduction

Water stable isotopes have been used for more than 40 years to study the hydrological cycle. With this goal, the International Atomic Energy Agency (IAEA) in Vienna and the World Meteorological Organisation in Geneva have set up a precipitation sampling network in the early 1960s to document the isotopic composition of precipitation, runoff and groundwaters. Two stable isotopes of hydrogen (^1H, D) and three stable isotopes of oxygen (^{16}O, ^{17}O, ^{18}O) can be found. The easiest molecules to measure (because of their abundance) are $H_2{}^{16}O$, $HD^{16}O$ and $H_2{}^{18}O$ and this is the reason why until very recently only the isotopic ratios $HD^{16}O/H_2{}^{16}O$ and $H_2{}^{18}O/H_2{}^{16}O$ were documented in the hydrological cycle.

Because of differences in mass and symmetry, each water phase change leads to a new distribution of the heavy to light molecules ratios in the different phases. This distribution is called fractionation and induces strong differences of the isotopic ratios for the different water cycle components (water vapor, liquid water, snow) at each phase transition of the hydrological cycle (e.g. evaporation, liquid condensation, snowflake formation). The main reason why the ratios $HD^{16}O/H_2{}^{16}O$ and $H_2{}^{18}O/H_2{}^{16}O$ are smaller in water vapor than in the condensed phase is that the heavy water molecules have a lower saturation vapor pressure than the light molecules. Such fractionation process due to saturation vapor pressure is called equilibrium fractionation. Additional fractionation of water also occurs in the vapor phase because of the different diffusivities of water molecules in air (the lightest molecules are also the fastest to diffuse). This fractionation process is usually depicted as kinetic fractionation. As an example, such kinetic fractionation enhances the depletion of heavy molecules in water vapor after the evaporation.

Liquid water condensation is mainly an equilibrium process. The stronger the condensation, i.e. the more important the distillation of the air mass, the more depleted in heavy isotopes the remaining water vapor. Condensation is enhanced for low temperature. Hence, this distillation mechanism leads to a decrease of the ratios $HD^{16}O/H_2{}^{16}O$ and $H_2{}^{18}O/H_2{}^{16}O$ in precipitation with decreasing temperature. In addition to this large influence of temperature on both the ratios $HD^{16}O/H_2{}^{16}O$ and $H_2{}^{18}O/H_2{}^{16}O$ via equilibrium fractionation during condensation, combined measurements of $HD^{16}O/H_2{}^{16}O$ and $H_2{}^{18}O/H_2{}^{16}O$ can bring complementary information on the evaporative conditions of the air mass. The reason for that is the strong influence of kinetic fractionation during evaporation and different sensitivities of the ratios $HD^{16}O/H_2{}^{16}O$ and $H_2{}^{18}O/H_2{}^{16}O$ to equilibrium and kinetic fractionations. Note that kinetic fractionation is also important during solid precipitation and thus influences d-excess as well. This aspect is discussed later in the text.

Water isotopes measurements have been largely

applied to the study of polar ice cores. Indeed, measurements of isotopic ratios in polar ice cores have made it possible to infer the variations of central Antarctic temperature over the last 800,000 years [1,2]. This is mainly the result of equilibrium fractionation during condensation as depicted above. Then, because of the different influence of the kinetic fractionation on the ratios $HD^{16}O/H_2{}^{16}O$ and $H_2{}^{18}O/H_2{}^{16}O$, combination of both measurements enables one to infer second order information on the history of the air mass and on conditions in the evaporative regions [3,4,5,6].

This second order parameter extracted from the combined measurements of the ratios $HD^{16}O/H_2{}^{16}O$ and $H_2{}^{18}O/H_2{}^{16}O$ is called deuterium excess and noted d-excess (see definition in section 2). It provides unique information on both temperature and relative humidity of the evaporative regions. Jouzel et al. [3] suggests strong variation of the relative humidity over the deglaciation based on the first d-excess record in a polar ice core (Dome C, East Antarctica). Then, using the long record of d-excess in the Vostok ice core, Vimeux et al. [4] evidenced the strong role of obliquity for controlling the temperature gradient between evaporative and polar regions. However, d-excess is not a simple parameter since it does not depend univocally on one climatic variable. As an example, Vimeux et al. [4] have shown how the temperature in the evaporative and in the polar regions, the isotopic composition and the relative humidity of the evaporative regions all contribute to d-excess.

Until very recently, $H_2{}^{17}O$ has not been measured in the hydrological cycle since no additional information was expected from this tracer compared to $H_2{}^{18}O$. Indeed, because of mass dependent fractionation in the hydrological cycle, the ratio $H_2{}^{17}O/H_2{}^{16}O$ was expected to change as 0.5 time the ratio $H_2{}^{18}O/H_2{}^{16}O$. However, recent experimental developments have made it possible to measure with high precision the ratios $H_2{}^{17}O/H_2{}^{16}O$ and $H_2{}^{18}O/H_2{}^{16}O$ in water. This analytical method is based on a fluorination reaction converting H_2O into O_2. Then, the isotopic composition of O_2 ($\delta^{17}O$ and $\delta^{18}O$) is measured by dual inlet on a mass spectrometer through 3 runs of 20 measurements [method detailed in 7].

With this method, it has been possible to evidence differences in the relationships between the ratios $H_2{}^{17}O/H_2{}^{16}O$ and $H_2{}^{18}O/H_2{}^{16}O$ for equilibrium (slope of 0.529±0.001) and kinetic fractionation processes (slope of 0.518±0.001) [7, 8]. Variation of the relative proportion of kinetic and equilibrium processes in the present-day hydrological cycle then explained why slight differences are observed in the relationship between the ratios $H_2{}^{17}O/H_2{}^{16}O$ and $H_2{}^{18}O/H_2{}^{16}O$ for different waters (leaf water, precipitation, water vapor) [9]. The combination of $H_2{}^{17}O/H_2{}^{16}O$ and $H_2{}^{18}O/H_2{}^{16}O$ in polar ice core is thus expected to give information on the air mass history in the same way that the dual measurements of $HD^{16}O/H_2{}^{16}O$ and $H_2{}^{18}O/H_2{}^{16}O$ can document the surface conditions of the evaporative ocean. Moreover, the influences of equilibrium and kinetic fractionation processes are different for the three ratios $H_2{}^{18}O/H_2{}^{16}O$, $H_2{}^{17}O/H_2{}^{16}O$ and $HD^{16}O/H_2{}^{16}O$. Thus, it is believed that adding the measurement of $H_2{}^{17}O$ to the usual measurements of $H_2{}^{16}O$, $H_2{}^{18}O$ and $HD^{16}O$ in ice cores will help to better document the evolution of the past hydrological cycle. In particular, Angert et al. [10] suggest that measurements of $H_2{}^{17}O$ can help in bringing information on the relative humidity of the evaporative regions.

Direct interpretation of the isotopic composition of ice core is difficult because it depends on the entire history of the moisture precipitating in the polar regions. It therefore integrates the fractionation processes during evaporation, transportation and precipitation. In order to best take into account all these steps, many modeling studies have been developed for isotopes in the hydrological cycle. First, simple models considers only one air mass trajectory, i.e. a unique source of moisture for snow precipitating in polar regions [11, 12, 13]. Then, they depict the different fractionation processes along this trajectory. The disadvantage of such models is that they do not consider the multiplicity of evaporative regions and the recharge of the air mass along the trajectory. However, they are very useful to perform sensitivity experiments and constrain the influence of each climatic variable on the isotopic composition of snow. Second, the incorporation of water isotopes in the Atmospheric General Circulation Models (AGCM) [e.g. 14, 15, 16] permits to consider the different source of moisture, the recharge of the air mass but does not permit to individualize the influence of one climatic parameter on the isotopic composition of surface snow.

In this chapter, the measurements of the abundances of the 4 water isotopes will be used to tentatively understand the past evolution of the hydrological cycle. In a first part, the basic definitions will be given for dealing with water isotopes in ice cores. In a second part, some results of isotopic variations in surface snow and ice cores in polar regions will be given and the variability of the water isotopic composition in space and back in time will be discussed. Finally, simple modeling approach will be presented in order to meaningfully interpret the spatial and temporal variations of the isotopic composition of water in ice of the polar regions.

2. Definitions

2.1 Delta notation and d-excess, $^{17}O_{excess}$ anomalies

High precision absolute measurements of isotopic ratios are difficult so that isotopic ratios are expressed as relative measurements with respect to a standard. Then, variations of the isotopic ratios $H_2{}^{18}O/H_2{}^{16}O$, $H_2{}^{17}O/H_2{}^{16}O$ and $HD^{16}O/H_2{}^{16}O$ are relatively small within the hydrological cycle. As a consequence, the isotopic composition of water is usually expressed using the delta (δ) notation as follows (example given for $H_2{}^{18}O/H_2{}^{16}O$):

$$\delta^{18}O = \left(\frac{(H_2{}^{18}O/H_2{}^{16}O)_{sample}}{(H_2{}^{18}O/H_2{}^{16}O)_{standard}} - 1 \right) \times 1000 \quad (1)$$

The standard for water measurements is the V-SMOW (Vienna Standard Mean Ocean Water).

When dealing with the 2 ratios $HD^{16}O/H_2{}^{16}O$ and $H^{18}O^{16}O/H_2{}^{16}O$, the measurements of the isotopic composition of meteoric water have shown that δD and $\delta^{18}O$ of precipitation are linearly related with a slope of about 8 ([17], Figure 1) so that:

$$\delta D = 8\delta^{18}O + 10 \quad (2)$$

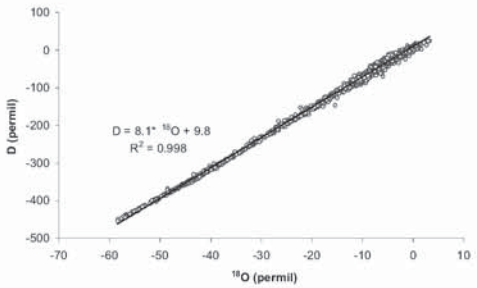

Figure 1: Repartition of δD and $\delta^{18}O$ of meteoric water. The data (annual average) are a compilation of the annual average of the GNIP (Global Network for Isotopes in Precipitation) network for $\delta^{18}O$ between -35 and 10‰ [18]. For the isotopic composition of Antarctic snow ($\delta^{18}O$ below -35‰), the data are from [19].

The slope of 8 for meteoric water in the δD – $\delta^{18}O$ plot mainly results from the fact that at equilibrium between liquid water and its vapor, the isotopic composition of the two phases lies on a line of slope close to 8. Then, the excess in deuterium, d-excess, was defined as [20]:

$$\text{d-excess} = \delta D - 8\delta^{18}O \quad (3)$$

The fact that d-excess is not equal to 0 in meteoric water of the temperate regions is mainly due to kinetic effects during evaporation of water and reevaporation of droplets. Note also that even without kinetic effect, a small d-excess exists in water because at equilibrium between liquid water and its vapor, the isotopic composition of the two phases lies on a line of slope close to 8 but not strictly equals to 8. As will be discussed later this slope depends on the temperature of the phase transition.

When dealing with fractionation between the three isotopes of oxygen, it has been chosen to express the isotopic composition with the logarithm expression [7, 10, 21] so that we will deal with the $\ln(\delta^{17}O/1000+1)$ – $\ln(\delta^{18}O/1000+1)$ system. In this system, the fractionation lines are straight. One disadvantage however is that the mixing lines are curved.

We present on Figure 2 a compilation of the isotopic composition of meteoric water in a $\ln(\delta^{17}O/1000+1)$ – $\ln(\delta^{18}O/1000+1)$ plot [9,22]. When drawing a regression line from these data, we end up with a slope of 0.528 (R^2=0.999999) and an intercept of 42 permeg (1 permeg = 10^{-3} per mil). This result is similar to the result by Meijer and Li [23]. Similarly to the situation in the δD-$\delta^{18}O$ system, the slope of 0.528 for the meteoric water line in the $\ln(\delta^{17}O/1000+1)$ – $\ln(\delta^{18}O/1000+1)$ system is primarily influenced by the process of equilibrium fractionation [7]. Then, as kinetic effects at evaporation are responsible for a significant residual d-excess in the meteoric water, the same effects explain why the intercept of the meteoric line with the line $\ln(\delta^{18}O/1000+1)=0$ is not equal to zero. Thus, based on the d-excess definition, we define the $^{17}O_{excess}$ as:

$$^{17}O_{excess} = \ln(\delta^{17}O/1000+1) - 0.528 * \ln(\delta^{18}O/1000+1) \quad (4)$$

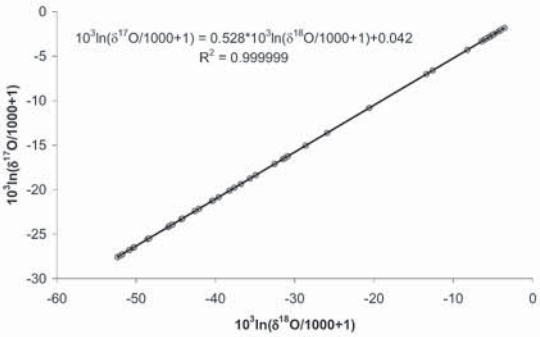

Figure 2: Repartition of the $\delta^{17}O$ and $\delta^{18}O$ of meteoric water [9; this sudy]. The values for Antarctica ($\delta^{18}O$<-35‰) come from the East Antarctica transect Terra Nova Bay – Dome C [24]. The other values are ground water from Israel and Europe [9].

From combined measurements of $\delta^{17}O$ and $\delta^{18}O$ through the fluorination technique described in details in [7], the analytical precision on $^{17}O_{excess}$ is of 5 permeg (see also the detailed discussion on $^{17}O_{excess}$ analytical precision in [9]).

We note here that slight differences still arise in the definitions of d-excess and $^{17}O_{excess}$. In particular, it is tempting to use the logarithm definition for d-excess or to define a $^{17}O_{excess}$ in a $\delta^{17}O$-$\delta^{18}O$ system. However, it can be shown that on a $\ln(\delta D/1000+1)$ – $\ln(\delta^{18}O/1000+1)$ plot, the repartition of the isotopic composition of the meteoric water is not along a unique line. Actually, the regression line for meteoric water in this system has a slope that increases between 8.4 and 10.5 for $\delta^{18}O$ decreasing between -10‰ (tropical - temperate regions) and -45‰ (polar regions). In this case, it is impossible to define univocally a d-excess over the entire range of isotopic composition of water. Similarly, if we display the isotopic composition of meteoric water in a $\delta^{17}O$-$\delta^{18}O$ plot instead of a $\ln(\delta^{17}O/1000+1)$ – $\ln(\delta^{18}O/1000+1)$ plot, the slope of the regression line is 0.535 for temperate regions and 0.539 for the polar regions while it remains 0.528 for all the different regions in a $\ln(\delta^{17}O/1000+1)$ –

$\ln(\delta^{18}O/1000+1)$ plot. Note that a change in the definition slope of $^{17}O_{excess}$ by 0.004 (from 0.535 to 0.539) leads to "artificial" variations of $^{17}O_{excess}$ by 20 permeg for a 5‰ change in $\delta^{18}O$. Typical variations of $^{17}O_{excess}$ defined on a logarithmic scale and with a slope of 0.528 are of the order of 20 permeg (analytical precision of 5 permeg). We therefore underline the importance of keeping the $^{17}O_{excess}$ definition in the $\ln(\delta^{17}O/1000+1) - \ln(\delta^{18}O/1000+1)$ system.

2.2 Fractionation coefficients

The variations of $\delta^{18}O$, δD and $\delta^{17}O$ in the hydrological cycle are due to fractionations at each phase transition. In order to quantify the fractionation of each process, fractionation coefficients, α, have been defined. As an example, we give the definition of $^{18}\alpha_{V\text{-}L}$ for the fractionation associated with the ratio $H_2{}^{18}O/H_2{}^{16}O$ during equilibrium between vapor and liquid (fractionation process associated with liquid precipitation):

$$ {}^{18}\alpha^{eq}_{V-L} = \frac{\left(H_2{}^{18}O / H_2{}^{16}O \right)_{liquid}}{\left(H_2{}^{18}O / H_2{}^{16}O \right)_{vapor}} \qquad (5) $$

Numerous laboratory experiments have been performed that enable the precise determination of the fractionation coefficients associated with equilibrium or kinetic fractionation at each phase transition and for the three isotopic ratios $H_2{}^{18}O/H_2{}^{16}O$, $H_2{}^{17}O/H_2{}^{16}O$ and $HD^{16}O/H_2{}^{16}O$. We give the values of the different fractionation coefficients as well as the references for their determination in Table 1.

It is interesting to compare here the evolution with temperature of the relationship between the equilibrium fractionation coefficients in the system $HD^{16}O/H_2{}^{16}O$ – $H_2{}^{18}O/H_2{}^{16}O$ and in the system $H_2{}^{17}O/H_2{}^{16}O$ – $H_2{}^{18}O/H_2{}^{16}O$. To do so, we display on Fig. 3, the evolution with temperature of the ratios $\ln^D\alpha^{eq}_{V\text{-}L}/\ln^{18}\alpha^{eq}_{V\text{-}L}$ and $\ln^D\alpha^{eq}_{V\text{-}S}/\ln^{18}\alpha^{eq}_{V\text{-}S}$ (Fig 3a) and the evolution with temperature of the ratios $\ln^{17}\alpha^{eq}_{V\text{-}L}/\ln^{18}\alpha^{eq}_{V\text{-}L}$ and $\ln^{17}\alpha^{eq}_{V\text{-}S}/\ln^{18}\alpha^{eq}_{V\text{-}S}$ (Fig 3b). While the ratios $\ln^{17}\alpha^{eq}_{V\text{-}L}/\ln^{18}\alpha^{eq}_{V\text{-}L}$ and $\ln^D\alpha^{eq}_{V\text{-}S}/\ln^{18}\alpha^{eq}_{V\text{-}S}$ are stable with temperature, the relationships between $\ln^D\alpha^{eq}_{V\text{-}L}$ and $\ln^{18}\alpha^{eq}_{V\text{-}L}$ or $\ln^D\alpha^{eq}_{V\text{-}S}$ and $\ln^{18}\alpha^{eq}_{V\text{-}S}$ clearly change with temperature (note that the same evolution could be observed for the ratios $({}^D\alpha^{eq}_{V\text{-}L}-1)/({}^{18}\alpha^{eq}_{V\text{-}L}-1)$ and $({}^D\alpha^{eq}_{V\text{-}S}-1)/({}^{18}\alpha^{eq}_{V\text{-}S}-1)$ which correspond more correctly to the d-excess definition). This will have important consequences in the compared interpretation of $^{17}O_{excess}$ and d-excess and especially explains why $^{17}O_{excess}$ should be less sensitive to temperature than d-excess.

Finally, note that we still lack from a direct experimental determination of $\ln^{17}\alpha^{eq}_{V\text{-}S}/\ln^{18}\alpha^{eq}_{V\text{-}S}$. This can lead to uncertainty in the results presented later and has therefore been taken into account in the discussion part.

	$H_2{}^{18}O/H_2{}^{16}O$	$H_2{}^{17}O/H_2{}^{16}O$	$HD^{16}O/H_2{}^{16}O$
$\ln\alpha^{eq}_{V\text{-}L}$	$\frac{1.137}{T^2}.10^3 - \frac{0.416}{T} - 2.07.10^{-3}$ [A]	$0.529\times\ln({}^{18}\alpha^{eq}_{V\text{-}L})$ [B]	$\frac{24.84}{T^2}.10^3 - \frac{76.25}{T} + 52.6.10^{-3}$ [A]
$\ln\alpha^{eq}_{V\text{-}S}$	$\frac{11.839}{T} - 28.224.10^{-3}$ [C]	$0.529\times\ln({}^{18}\alpha^{eq}_{V\text{-}L})$ [D]	$\frac{16288}{T^2} - 9.34.10^{-2}$ [E]
$\ln\alpha^{k}$	0.0122 [F]	$0.518\times\ln({}^{18}\alpha^{k})$ [G]	0.01077 [F]

Table 1: Compilation of the fractionation coefficients and associated references.
$\alpha^{eq}_{V\text{-}L}$ is the fractionation coefficient associated with vapor-liquid equilibrium; $\alpha^{eq}_{V\text{-}S}$ is the fractionation coefficient associated with vapor-solid equilibrium; α^{k} is the fractionation coefficient associated with kinetic effect (diffusion of water vapor in air).
A: Experimental determination by [25].
B: Experimental determination by [7] in the range 10-40°C in agreement with theoretical determination by [26].
C: Experimental determination by [27].
D: Theoretical determination by [26]
E: Experimental determination by [28]
F: Experimental determination by [29]
G: Experimental determination by [8]

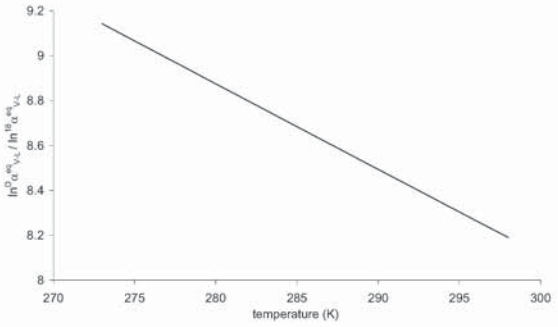

Figure 3a: Evolution of $\ln^D\alpha^{eq}_{V\text{-}L}/\ln^{18}\alpha^{eq}_{V\text{-}L}$ with temperature.

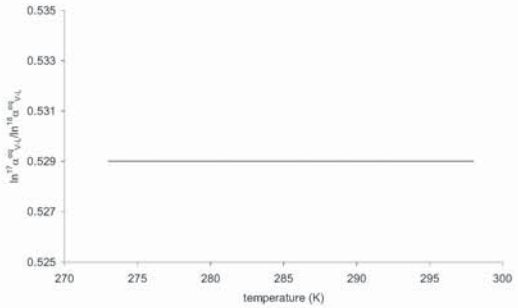

Figure 3b: Evolution of $\ln^{17}\alpha^{eq}_{V\text{-}L}/\ln^{18}\alpha^{eq}_{V\text{-}L}$ with temperature.

3. Spatial and temporal distribution of isotopic composition of water in the polar regions

3.1 Spatial distribution of the isotopic composition of water in surface snow

As stated in the introduction, it has long been observed that the stable isotopic composition of precipitation at high latitudes ($\delta^{18}O$, $\delta^{17}O$ or δD) is primarily related to surface air temperature [17]. In Antarctica, surface snow was sampled along traverses from the coastal to inland stations and firn temperature measurements used as indicators of annual mean surface temperature. From these measurements, studies were conducted to determine the spatial relationship between precipitation isotopic composition and local temperature (isotopic thermometer) [30]. Recently, [19] compiled isotopic measurements over 1000 locations in Antarctica and determined the following global slopes for the isotopic thermometer in Antarctica: 0.80±0.01‰ per °C for $\delta^{18}O$ and 6.33±0.09‰ per °C for δD. The slope increases by ~20% at high elevation locations such as on the East Antarctica plateau.

We focus now on the compared distribution of d-excess and $^{17}O_{excess}$ in Antarctic surface snow. We present on Figure 4 the evolution of d-excess and $^{17}O_{excess}$ measured on surface snow along an East-Antarctica transect between Terra Nova Bay (74.7°S 159.7°E) and Dome C (75.1°S 123.4°E) [19, 22]. d-excess increases significantly with decreasing $\delta^{18}O$ over the East Antarctica plateau (i.e. $\delta^{18}O$ lower than –35‰) while $^{17}O_{excess}$ remains constant (40 per meg) over the entire transect. Such contrasted spatial evolutions between d-excess and $^{17}O_{excess}$ are rather surprising given the similarities in the definition of the two "excess".

It is important to note that the scatter of the data along the transect is relatively large, and is greater than our analytical precision shown by the error bars on Fig. 4. Many reasons can explain such a scattering such as variations of source and trajectories for the different surface snow samples, snow redistribution by wind, uneven deposition due to snow relief forms of various scales, post-deposition effects (mainly associated with kinetic effects and thus believed to strongly modify $^{17}O_{excess}$ and d-excess [24, 31, 32]).

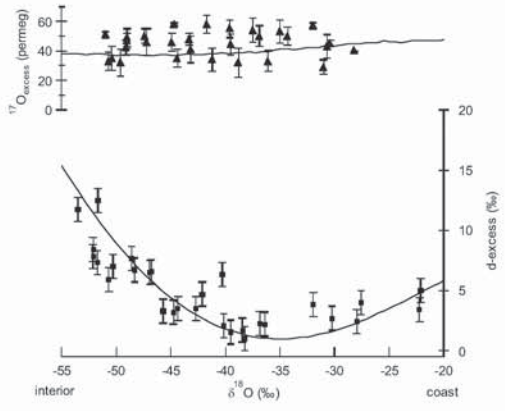

*Figure 4: Repartition of d-excess, $^{17}O_{excess}$ and $\delta^{18}O$ along an Antarctic transect between Terra Nova Bay (on the coast) and Dome C (East Antarctic plateau). d-excess data are from [19]. The solid lines show the output of the MCIM (see main text) tuned with a supersaturation S_i=1-0.002*T.*

3.2 Temporal variations of δD, d-excess and ^{17}O-excess over the last deglaciation in the Vostok station (East Antarctica)

Figure 5 displays a rough profile of δD, $\delta^{18}O$, d-excess [4], $\delta^{17}O$ and $^{17}O_{excess}$ [22] over the last deglaciation from the Vostok ice core (78°27′S, 106°52′E). At first order, δD, $\delta^{17}O$ and $\delta^{18}O$ show the same increasing signal so that we discuss only the δD record. The δD profile shows a clear increase between the last glacial maximum (LGM) and the Holocene by 50‰, a magnitude common to all continental Antarctic ice cores, that reflects the general warming over the deglaciation [33]. d-excess and $^{17}O_{excess}$ have both a general tendency of increase over the deglaciation but while the d-excess decreases slightly from 30 kyrs and reaches its minimum value around 15 kyrs BP, $^{17}O_{excess}$ remains stable between 30 and 20 kyrs BP around 15-20 permeg and increases over the deglaciation up to 40 permeg. Again, despite similarities in the definition of d-excess and $^{17}O_{excess}$, their temporal evolutions are clearly different. Hence, we discuss below the origin of d-excess and $^{17}O_{excess}$ in order to explain these different evolutions and thus to extract the maximum of information from these two signals.

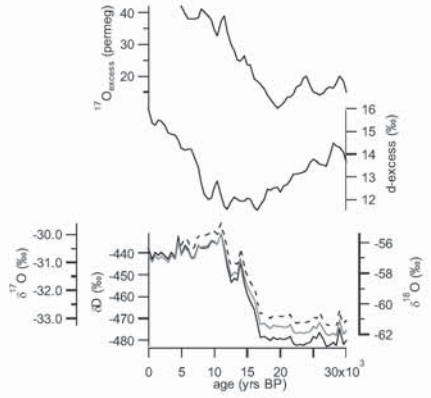

Figure 5: Evolution of δD [Vimeux et al., 1999, $\delta^{17}O$ (dashed line) [22], $\delta^{18}O$ (grey) [4; 22], $^{17}O_{excess}$ [22] and d-excess [4] during the deglaciation. Data were interpolated every 500 years.

4. The origin of the signature of d-excess and $^{17}O_{excess}$ in polar ice

In this section, we will describe the major steps of the hydrological cycle. We will also discuss how fractionation associated with each step can modify d-excess and $^{17}O_{excess}$ in polar snow and thus explain the spatial and temporal variabilities of d-excess and $^{17}O_{excess}$ depicted in the previous section.

4.1 Evaporation: the isotopic composition of the first vapor

During evaporation or reevaporation of water into an unsaturated atmosphere, there is no thermodynamic equilibrium between the liquid and the vapor phases. In this case, it is necessary to consider both the equilibrium isotopic fractionation and the so-called kinetic fractionation due to molecular diffusivities of the isotopically different water molecules in air.

The combination of equilibrium and kinetic effects during evaporation is actually the origin of an anomaly (d-excess or $^{17}O_{excess}$) in the vapor over the ocean. We illustrate this effect on Fig. 6 both on a δD-$\delta^{18}O$ plot and on a $\ln(\delta^{17}O/1000+1) - \ln(\delta^{18}O/1000+1)$ plot. The departure point is the oceanic water with the average water isotopic composition of VSMOW, hence with δD, $\delta^{18}O$ and $\delta^{17}O$ equals to 0‰.

The effect of pure equilibrium fractionation would be to drive the isotopic composition of the water vapor toward lower $\delta^{18}O$ (~ -10‰) along a slope of ~8 in the δD-$\delta^{18}O$ system and 0.528 in the $\ln(\delta^{17}O/1000+1) - \ln(\delta^{18}O/1000+1)$ system. These slopes are simply the result of the ratios of the fractionation coefficients (expressed in ln) given in Table 1: for the δD-$\delta^{18}O$ system, the ratio $\ln^{D}\alpha^{eq}_{V\text{-}L}/\ln^{18}\alpha^{eq}_{V\text{-}L}$ varies with temperature between 9 and 8 in the range 0-25°C (Fig. 3a) and for the $\ln(\delta^{17}O/1000+1) - \ln(\delta^{18}O/1000+1)$ system, the ratio $\ln^{17}\alpha^{eq}_{V\text{-}L}/\ln^{18}\alpha^{eq}_{V\text{-}L}$ remains stable and equal to 0.529 with varying temperature (Fig. 3b, [7]).

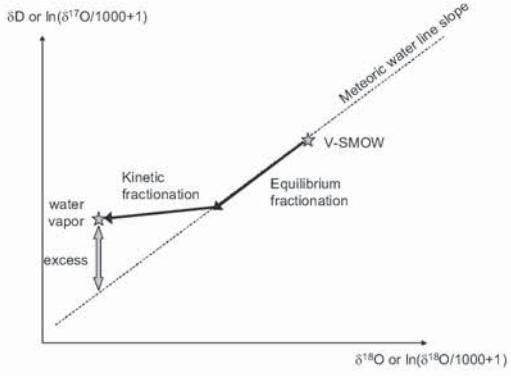

Figure 6: Scheme showing the isotopic composition of the first water vapor over the ocean. The departure point is the ocean with the isotopic composition of V-SMOW. Equilibrium fractionation has a slope close to the one of the meteoric water line.
1- Note that the true meteoric water line (not presented here) does not go through V-SMOW because it has a d-excess and a $^{17}O_{excess}$ different from zero. We present here a parallel of the meteoric water line, i.e. a line with the slope of the meteoric water line but with an intercept of zero for $\delta^{18}O=0$.
2- Note that for the system $\ln(\delta^{17}O/1000+1) - \ln(\delta^{18}O/1000+1)$, we exaggerate the differences between the slopes for equilibrium (0.529) and kinetic (0.518) fractionation processes.

In addition to the equilibrium fractionation, the effect of kinetic fractionation is to drive the isotopic composition of the water vapor along a lower slope: 0.88 ($=\ln^{D}\alpha^{k}_{V\text{-}L}/\ln^{18}\alpha^{k}_{V\text{-}L}$) for the δD-$\delta^{18}O$ system and 0.518 ($=\ln^{17}\alpha^{k}_{V\text{-}L}/\ln^{18}\alpha^{kq}_{V\text{-}L}$) for the $\ln(\delta^{17}O/1000+1) - \ln(\delta^{18}O/1000+1)$ system [8]. Fig. 6 shows that the effect of kinetic fractionation is to drive the isotopic composition of the water vapor away from the line of slope 8 for the system δD-$\delta^{18}O$ and 0.528 for the system $\ln(\delta^{17}O/1000+1)$-$\ln(\delta^{18}O/1000+1)$. From this scheme, it is clear that the more important the relative proportion of kinetic effect with respect to equilibrium effect, the more important the d-excess and the $^{17}O_{excess}$.

We detail below how the kinetic effect can be increased at evaporation. The classical description used to quantify the isotope effects accompanying evaporation into an unsaturated atmosphere was first formulated by [34]. It states that the isotopic composition of the net evaporation flux depends mainly on the environmental parameters controlling the evaporation process, i.e. relative humidity above the boundary layer, and isotopic composition of the surrounding water vapor. Then, Brutsaert [35, 36] proposed a more sophisticated model for the evaporation of water incorporating the effect of surface wind speeds. [29] showed that this model was in good agreement with observed fractionation for various wind tunnel laboratory experiments. At first order, the main effect is the one of relative humidity (RH): if RH decreases, the importance of diffusion increases and a large kinetic fractionation effect is observed that drives large increase of d-excess and $^{17}O_{excess}$.

For a quantitative approach of this effect, we follow the previous work by [37] assuming a steady state during evaporation so that the net fluxes of evaporation equals the net flux of precipitation on a global scale. In this case, the isotopic composition of the water vapor above the ocean is given by:

$$\delta^{*}_{V} = {}^{*}\alpha_{V\text{-}L} \times \frac{1-k^{*}}{1-k^{*}\times \mathrm{RH}} - 1 \qquad (6)$$

where * stands for D, ^{17}O or ^{18}O, $\alpha_{V\text{-}L}$ is the isotopic equilibrium fractionation coefficient at the ocean surface temperature and k^{*} is a parameter describing the diffusion fractionation effects at the air-ocean boundary. Note that in this equation, it is assumed that the ocean has the same isotopic composition as the VSMOW standard.

The vapor-liquid fractionation factors are given in Table 1. Based on estimates of wind speed over the ocean, it was suggested that the values of $k^{18}O$ corresponding to ocean surface evaporation regime over the last climatic cycle vary in the range 4.5-6‰ [3; 38]. From Table 1, we have $k^{D}/k^{18}=0.88$ and $k^{17}/k^{18} = 0.518$.

From Eq. 6, it is now possible to infer the influence of relative humidity (RH) on the isotopic composition of the first water vapor over the ocean. However, because $\alpha_{V\text{-}L}$ depends on temperature (Table 1), sea surface

temperature (SST) has also an influence on this first water vapor isotopic composition. Hence, we present on Fig. 7 a comparison of d-excess and $^{17}O_{excess}$ of the water vapor for different relative humidities and temperatures. For decreasing RH, both $^{17}O_{excess}$ and d-excess increase while for increasing temperature, only d-excess increases ($^{17}O_{excess}$ remains stable). The reason why SST influences much less $^{17}O_{excess}$ than d-excess is that the ratio $\ln(^{17}\alpha_{V\text{-}L})/\ln(^{18}\alpha_{V\text{-}L})$ does not vary with temperature while $\ln(^{D}\alpha_{V\text{-}L})/\ln(^{18O}\alpha_{V\text{-}L})$ does (Fig. 3).

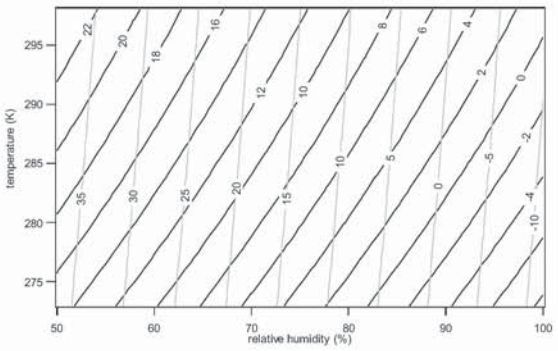

Figure 7: Evolutions of d-excess (black) and $^{17}O_{excess}$ (grey) of the first vapor for different temperatures and relative humidities. These evolutions were calculated from Eq. 6 with a diffusive coefficient k=5.25‰ (arbitrary chosen in the middle of the possible range for k, i.e. 4.5 to 6‰).

Finally, we should also consider deviation from the steady state approach described above. In particular, it has been shown that the validity of the closure assumption described above decreases as a region obtains a greater fraction of moisture from external sources [39]. The best way to correctly take into account the multiplicity of source region for the air moisture is to use Atmospheric General Circulation Model (AGCM) with the incorporation of water isotopes [e.g. 40; 41]. Such approach is not yet done for $\delta^{17}O$ and is beyond the scope of this chapter.

4.2 Liquid precipitation: isotopic composition of rain

After the first stage of evaporation, the parcel of humid air is transported from the evaporative regions to the polar regions. Since the air is cooling during its ascend after evaporation and transportation toward the high latitudes, it reaches at some point the dew point and condensation occurs. During the first part of the air parcel transportation, liquid precipitation occurs. According to measurements performed in surface air moisture and precipitation [42; 43; 44], the rain is considered at equilibrium with the water vapor so that the liquid precipitation process is assumed to occur at liquid-vapor equilibrium.

The removal of water through the liquid precipitation process is associated with progressive isotopic depletion of the remaining water vapor in the air parcel. This is usually described by the Rayleigh process. We do not develop here the basic approach for isotopic enrichment and depletion by the Rayleigh distillation that has been largely developed elsewhere [e.g. 20; 45]. We only give the final integral form to express the isotopic composition of the liquid water precipitating as a function of the fraction, f, of the water remaining in the air parcel (1 after the first evaporation, 0 when all water within the parcel is precipitated):

$$\ln R = \ln R_0 + (\alpha_{V\text{-}L}-1) \times \ln f \qquad (7)$$

where R is the isotopic ratio of heavy to light molecules of the precipitating water and R_0 the initial isotopic ratio of heavy to light molecules of the water vapor after first evaporation. Note that in this final form, α is assumed to be constant, i.e that temperature is constant along the distillation process.

From Eq. 7, it can be calculated how liquid precipitation modifies d-excess and $^{17}O_{excess}$ of the precipitating water (Table 2). Because $\ln(^{17}\alpha_{V\text{-}L})/\ln(^{18}\alpha_{V\text{-}L})$ equals 0.529 and does not depend on the temperature, it follows that $^{17}O_{excess}$ does not show significant changes between the first vapor over the ocean and the precipitating liquid water. On the contrary, the fact that $\ln(^{D}\alpha_{V\text{-}L})/\ln(^{18}\alpha_{V\text{-}L})$ shows significant variations with temperature leads to large differences of d-excess in the precipitating liquid water at different temperatures. It should be mentioned that similar results are found if we consider variations in the temperature along the distillation process. This has important implication for the d-excess interpretation. Indeed, because of the strong influence of temperature on d-excess during the liquid precipitation process, it results that the main influence on polar d-excess is not relative humidity (that has a strong influence on the first vapor) but the temperature in the source regions [12].

T	F	$\delta^{18}O$ (‰)	d-excess (‰)	$^{17}O_{excess}$ (permeg)
283	0.9	-12.06	8.2	10
283	0.6	-16.31	7.2	11
276	0.9	-12.14	7.9	10
276	0.6	-16.71	5.4	12

Table 2: Evolution of $\delta^{18}O$, d-excess and $^{17}O_{excess}$ along a distillation trajectory considering only liquid precipitation. The isotopic composition of the initial vapor was arbitrary chosen as $\delta^{18}O$=-11.05‰, d-excess=8.8 ‰, $^{17}O_{excess}$ = 10 permeg.

Note that in addition to the liquid precipitation process at equilibrium, there are evidences of rain reevaporation in the tropical and temperate regions [20; 44]. Reevaporation of rain in tropical regions has the potential to modify the isotopic composition of the air mass [46; 47]. This is largely associated with kinetic fractionation [Dansgaard, 1964]. The effect of reevaporation on $^{17}O_{excess}$ and d-excess is difficult to quantify but it can be schematized as follows. First, increasing the rain reevaporation fraction in moist convective clouds leads to an initial decrease of the air

mass $\delta^{18}O$ [46] and then, for a constant RH, the associated $^{17}O_{excess}$ and d-excess largely increase in vapor. However, RH is not expected to remain constant. More reevaporation should lead to enhance RH and thus to a decrease of d-excess and $^{17}O_{excess}$ in the water vapor. Because of the complexity in depicting the isotopic effect due to reevaporation, it is often not incorporated in isotopic models of the hydrological cycle.

4.3 Solid precipitation

When the temperature decreases below a certain threshold, ice crystals can form in the atmosphere and solid precipitation occurs. Isotopic fractionation associated with solid precipitation has been studied by [11]. They showed that snow formation is not at equilibrium and that kinetic effects are to be considered in the vapor to snow sublimation process. In this approach, the relative proportion of kinetic effect during solid precipitation depends on the supersaturation in polar clouds and the effective fractionation factor in the sublimation process is expressed as:

$$\alpha = \alpha_k \times \alpha_{V\text{-}S} \quad (8)$$

With $\alpha_{V\text{-}S}$ the fractionation coefficient for the solid-vapor equilibrium and α_k defined as:

$$\alpha_k = \frac{S_i}{1+\alpha_{V-S}(S_i-1)D/D'} \quad (9)$$

D and D' being the diffusion constants in air for the light and the heavy isotopic components respectively. The ratio D/D' is 1.0285 for $H_2{}^{18}O$, 1.0251 for HDO [29] and 1.01466 for $H_2{}^{17}O$ (calculated from [9]). S_i is the supersaturation ratio in polar clouds and [11] showed that adjusting S_i as a linear function of the inversion temperature permits to explain the isotopic composition of polar snow. Note that using the values D/D' determined by [48] would not change the results of our modeling studies discussed below (the supersaturation would simply be tuned differently).

Using a Rayleigh process description, it is possible to evaluate the isotopic composition of the falling snow [11]. To do so, S_i needs to be precisely constrained. This is usually done through the following approach first given by [12] and detailed by [49] for the transect between Dumont d'Urville and Dome C: a complete model based on the Rayleigh distillation process is developed for the air parcel transportation and isotopic fractionation is calculated at each step between the evaporation over the ocean and the final polar precipitation. Then, S_i is tuned so that the modeled isotopic composition of polar snow matches the measurements.

We followed this method using the mixed clouds isotopic model (MCIM) by [13] in which we incorporated the description of $H_2{}^{17}O$ in the different steps of the hydrological cycle as described above. In a first approximation, we assume a unique source evaporative region for all precipitation along the Antarctica transect (from the coast to the East Antarctica plateau). To identify the climatic parameters associated with this evaporative region, we used the AGCM results of [41] that permitted to identify the different source regions for the snow precipitating in Antarctica. For East Antarctica, they found that the major contributors are the Austral Ocean and the Southern Indopacific Ocean. From these results, we can roughly calculate that the oceanic source for the Antarctic precipitation has a temperature around 17°C and a relative humidity RH around 80% (associated uncertainty of 30% of the estimate). Finally, we adjusted the supersaturation S_i using the $\delta^{18}O$, d-excess and $^{17}O_{excess}$ data over the East-Antarctic transect between Terra Nova Bay and Dome C (Fig. 4). A supersaturation S_i=1-0.002×T was chosen to best fit our measurements. This parameterization of supersaturation is comparable to the previous studies [12; 13; 49; 50]. We believe that such parameterization is rather robust since it is based on the tuning on $\delta^{18}O$, d-excess and $^{17}O_{excess}$ data opposite to the previous studies for which only $\delta^{18}O$ and d-excess measurements were available.

Note that our first order assumption that all the water precipitating along the Antarctic transect is issued from the same evaporative source is very unlikely. Actually, results from reanalysis [51] and modeling outputs [41, 52] show that the coastal regions from East Antarctica such as Terra Nova Bay, receive more moisture from the Antarctic current while the inner regions from East Antarctica, hence Dome C, receive more moisture from the Southern Indopacific. Using modeling outputs by [41], we calculated that the moisture source for Terra Nova Bay has a mean temperature of roughly 15°C and a mean RH of ~ 80% while the moisture source for Dome C has a mean temperature of 18°C and the same mean RH of 80%. These figures are only very rough estimates based on modeling studies and should only be considered as rough estimates (associated uncertainty of 30%). Based on these results, we estimated the implications of this change in the source location for our modeling: we found that our modeled d-excess presented in Fig. 4 is overestimated by up to 0.7‰ on the coastal site and underestimated by up to 1.4‰ in the inner site. $^{17}O_{excess}$ is not influenced by the change in source region because the source RH remains the same (in the model estimates). These variations in d-excess remain however within the scattering of the data so that we consider that the aforementioned parameterization of our simple model is valid. Note that in this simple approach, we did not consider additional potential effects such as the seasonality of the precipitation and post-deposition effects that are probably different between the coast and the interior of Antarctic.

Finally, it should be noted that $^{17}O_{excess}$ measured in Antarctic snow is significantly larger than $^{17}O_{excess}$ in the first vapor as modeled by the closure assumption of [37]. Several reasons may explain such discrepancy. First, we lack from data of $^{17}O_{excess}$ in the Southern Indopacific

Ocean and it should be checked that $^{17}O_{excess}$ in this ocean is 0 permeg. Second, in our application of the closure assumption, we have displayed the evolution of $^{17}O_{excess}$ with respect to relative humidity to be coherent with the previous approaches of [4; 13; 37] but it is perhaps more correct to use the normalized relative humidity [e.g. 53] – i.e. water-air mixing ratio in the free atmosphere divided by the same ratio in air in equilibrium with the ocean surface. In this case, $^{17}O_{excess}$ of the first vapor is increased by 10-20 permeg [22].

4.4 Final influences on polar d-excess and $^{17}O_{excess}$

We used the simple MCIM model described above (without including effects of reevaporation) and the tuning on the Antarctic transect to determine the different influences on ice $\delta^{18}O$, $^{17}O_{excess}$ and d-excess of temperature, RH and isotopic composition of seawater of the source region (T_{source}, RH_{source} and $\delta^{18}O_{ocean}$) and temperature of the polar region (T_{site}). We ran several hundreds of sensitivity experiments and we summarized the different influences on d-excess and $^{17}O_{excess}$ at the Vostok station as follows:

$$\Delta\text{d-excess (‰)} = -1.0\times\Delta T_{site} + 1.4\times\Delta T_{source} - 0.12\times\Delta RH_{source} - 3\times\Delta\delta^{18}O_{ocean} \quad (10)$$

$$\Delta^{17}O_{excess}\text{ (permeg)} = -0.9\times\Delta RH_{source} \quad (11)$$

$$\Delta\delta^{18}O\text{ (‰)} = 1.15\times\Delta T_{site} - 0.5\times\Delta T_{source} + 0.15\times\Delta RH_{source} + 0.95\times\Delta\delta^{18}O_{ocean} \quad (12)$$

where Δ stands for the deviation from the present-day conditions. Note that the use of the transect between Terra Nova Bay and Dome C is probably not optimal to determine the influences on the isotopic composition of surface snow in Vostok and surface data around Vostok are strongly needed. However, additional measurements not shown here depict the same change in $^{17}O_{excess}$ over the deglaciation in Dome C as in Vostok so that the conclusions drawn here are believed to be valid for the whole East Antarctic plateau.

The reason why d-excess depends on the isotopic composition of the surface ocean, $\delta^{18}O_{ocean}$, and not $^{17}O_{excess}$ is that the $^{17}O_{excess}$ is defined using the "ln" operation while the definition of d-excess does not include the "ln". This can be easily shown by the approach of [54] studying the influence of $\delta^{18}O_{ocean}$ on the isotopic composition of polar snow. In a Rayleigh model describing the isotopic behavior of an air mass from its oceanic origin to the precipitation site, the isotopic content of precipitation (here $\delta^{18}O_{ice}$) can be written:

$$1+\delta^{18}O_{ice} = {}^{18}F(1+\delta^{18}O_{ocean}) \quad (13)$$

where ^{18}F is a function of climatological parameters and fractionation coefficients for the system $H_2{}^{18}O/H_2{}^{16}O$. Applying this equation for present-day ($\delta^{18}O_{ocean}(0)$) and for a certain period in the past, $\delta^{18}O_{ocean}(t)=\delta^{18}O_{ocean}(0)+\Delta\delta^{18}O_{ocean}$, shows that the correction due to the surface ocean isotopic composition equals

$$^{18}F\times\Delta\delta^{18}O_{ocean}=\Delta\delta^{18}O_{ocean}\times(1+\delta^{18}O_{ice})/(1+\Delta\delta^{18}O_{ocean}) \quad (14)$$

We do the reasonable assumption that d-excess of the surface ocean remains nil in the past. Then, the correction for d-excess due to isotopic composition of the ocean equals

$$\text{Corr\_d-excess} = 8\times\Delta\delta^{18}O_{ocean}\times\left(\frac{1+\delta D_{ice}}{1+8\Delta\delta^{18}O_{ocean}} - \frac{1+\delta^{18}O_{ice}}{1+\Delta\delta^{18}O_{ocean}}\right) \quad (15)$$

Similarly we can express the correction due to the surface ocean for $^{17}O_{excess}$ and we find

$$\text{Corr\_}{}^{17}O_{excess} = \ln(F_{17}\times(1+\delta^{17}O_{ocean})) - 0.528\times\ln(F_{18}\times(1+\delta^{18}O_{ocean})) - \ln F_{17} + 0.528\times\ln F_{18} \quad (16)$$

If $^{17}O_{excess}$ of the ocean remains nil, it follows that this correction equals zero so that no term including $\Delta\delta^{18}O_{ocean}$ appears in equation (11).

Equations (10), (11) and (12) were obtained with a particular parameterization of the model (S_i, fraction of condensed phase that remains in the cloud,…) but other sets of parameters enable one to obtain a similar agreement with the surface data. Moreover the ratio of fractionation factors $\ln{}^{17}\alpha^{eq}_{V\text{-}S}/\ln{}^{18}\alpha^{eq}_{V\text{-}S}$ has not been checked experimentally. We therefore did sensitivity experiments exploring randomly the range of parameters involved in the simple isotopic model and making $\ln{}^{17}\alpha^{eq}_{V\text{-}S}/\ln{}^{18}\alpha^{eq}_{V\text{-}S}$ vary by ± 0.005. We retain only the parameterizations allowing to fit the $^{17}O_{excess}$ and d-excess data of Fig. 4 (square root of the mean square deviation < 15 permeg for $^{17}O_{excess}$ and < 3‰ for d-excess). In this case, the influence of T_{source} on $^{17}O_{excess}$ remains negligible and we find a maximum influence of T_{site} on $^{17}O_{excess}$ of -0.8 permeg/°C. The uncertainty associated with the other coefficients in Eq. 10, 11 and 12 is of 20%. Finally, note that coefficients in Eq. 10 and 12 are of the same order of magnitude than the equations obtained by [55] for Vostok and [5] for the Dome C ice core which confirm the robustness of our approach.

5. Discussion and conclusion

From the analysis above, we are now able to propose several hypotheses to explain the changes in d-excess and in $^{17}O_{excess}$ between the LGM and the Holocene.

We have shown that the $^{17}O_{excess}$ is neither

influenced by temperature, nor by the isotopic composition of the surface ocean. Therefore, the increase of $^{17}O_{excess}$ during the deglaciation is probably only due to increase in the kinetic effect at evaporation or reevaporation. The modeling study of section 4-4 suggests that this increase can be driven by a decrease in relative humidity in the evaporative regions. Eq. 11 suggests that a decrease by more than 20% of relative humidity of the evaporative regions is needed to explain the $^{17}O_{excess}$ increase over the deglaciation. Note that [3] also suggested a higher relative humidity during the last glacial maximum based on ice d-excess interpretation but the difference was only of 10% with respect to present-day. A higher relative humidity over the ocean in the glacial is not unexpected since saturation is reached more easily for lower temperature. Based on a compilation of atmospheric general circulation model results, [56] showed that RH is indeed expected to increase from 80 to 90% over the ocean when the sea surface temperature decreases from 20 to 10°C. However, a 20% change of relative humidity over the ocean during the deglaciation is clearly too high and we should search for other explanations for this $^{17}O_{excess}$ signal. One possibility is an increase of the reevaporation of liquid precipitation over the deglaciation that will increase the water vapor $^{17}O_{excess}$ (section 4-2).

For the d-excess signal, the same causes can be invoked since the increase of kinetic effects at evaporation and reevaporation increases both d-excess and $^{17}O_{excess}$ in the vapor. However, temperature and isotopic composition of surface seawater were shown to influence d-excess as well. $\Delta\delta^{18}O_{ocean}$ is expected to be 1‰ for the LGM and source temperature probably changed as well so that part of the shift in d-excess between the LGM and the Holocene can be explained by the changes in isotopic composition of seawater and in sea surface temperature over the deglaciation [55].

Finally, when comparing the different possible influences on d-excess and $^{17}O_{excess}$, it appears that d-excess is a more complex parameter than $^{17}O_{excess}$. Indeed, while $^{17}O_{excess}$ seems to depend only on the relative proportion of kinetic effect in the source regions, d-excess is strongly influenced by temperature and isotopic composition of seawater. Such differences in the influences of polar d-excess and $^{17}O_{excess}$ explain the observed dissimilarities in the evolutions of both parameters (Fig. 4 and 5).

A perspective for the future is to combine d-excess and $^{17}O_{excess}$ measurements in polar ice cores in order to decipher the influence of relative humidity and temperature and thus reconstruct quantitative information about the past changes in the hydrological cycle. It is tempting to do such exercise based on equations (10), (11) and (12). However, the large RH_{source} variation necessary to explain our $^{17}O_{excess}$ signal (20%) are not realistic and underline the current limitation in our understanding of isotopes repartition in the hydrological cycle.

In order to better understand the $^{17}O_{excess}$ signal, it is therefore key to progress toward different directions. First, it is obvious that the relative proportion of equilibrium and kinetic fractionation effects is not only controlled by relative humidity over the ocean and it is important to understand what drives $^{17}O_{excess}$ variations in the water vapor over the ocean; measurements of $^{17}O_{excess}$ in the boundary layer are thus strongly needed. Second, kinetic fractionation processes are believed to be important in the tropical regions due to reevaporation and convection effects. Studies of $^{17}O_{excess}$ in these regions are thus of high interest. Finally, we have shown the limitation of 1D simple isotopic modeling of the water cycle. Integration of $H_2{}^{17}O$ in atmospheric general circulation models is therefore an important step to go further in the understanding of $^{17}O_{excess}$ repartition in the hydrological cycle.

References

[1] EPICA members, "Eight glacial cycles from an Antarctic ice core", Nature, 429, 2004, pp. 623-627.

[2] J. Jouzel, V. Masson-Delmotte, O. Cattani, G. Dreyfus, S. Falourd, G. Hoffmann, B. Minster, J. Nouet, J.M. Barnola, J. Chappellaz, H. Fischer, J.C. Gallet, S. Johnsen, M. Leuenberger, L. Loulergue, D. Luethi, H. Oerter, F. Parrenin, G. Raisbeck, D. Raynaud, A. Schilt, J. Schwander, E. Selmo, R. Souchez, R. Spahni, B. Stauffer, J.P. Steffensen, B. Stenni, T.F. Stocker, J.L. Tison, M. Werner and E.W. Wolff, "Orbital and Millennial Antarctic Climate Variability over the Past 800,000 Years", Science, 317. no. 5839, 2007, pp. 793 – 796.

[3] J. Jouzel, L. Merlivat, L. and C. Lorius, "Deuterium excess in East Antarctic ice core suggests higher relative humidity at the oceanic surface during the last glacial maximum", Nature, 299, 1982, pp. 686-691.

[4] F. Vimeux, V. Masson, J. Jouzel, M. Stievenard, and J.R. Petit, "Glacial-interglacial changes in ocean surface conditions in the Southern Hemisphere", Nature, 398, 1999, pp. 410-413.

[5] B. Stenni, V. Masson-Delmotte, S. Johnsen, J. Jouzel, A. Longinelli, E. Monnin, R. Röthlisberger, and E. Selmo, An oceanic cold reversal during the last deglaciation, Science, 293, 2001, pp. 2074-2077.

[6] V. Masson-Delmotte, A. Landais, M. Stievenard, O. Cattani, S. Falourd, J. Jouzel, S.J. Johnsen, D. Dahl-Jensen, A. Sveinsbjornsdottir, J.W.C. White, T. Popp and H. Fischer, "Holocene climatic changes in Greenland: Different deuterium excess signals at Greenland Ice Core Project (GRIP) and NorthGRIP", J. Geophys. Res., 110 (D14101), 2005, doi:10.1029/2004JD005575.

[7] E. Barkan and B. Luz, "High precision measurements of $^{17}O/^{16}O$ and $^{18}O/^{16}O$ of O_2 in H_2O". Rapid Commun. Mass. Spec., 19, 2005, pp. 3737-3742.

[8] E. Barkan and B. Luz, "Diffusivity fractionations of $H_2^{16}O/H_2^{17}O$ and $H_2^{16}O/H_2^{18}O$ in air and their implications for isotope hydrology", Rapid Communication in Mass Spectrometry, 21, 2007, pp. 2999-3005.

[9] A. Landais, E. Barkan, D. Yakir and B. Luz, "The triple isotopic composition of oxygen in leaf water", Geochim. Cosmochim. Acta, 70, 2006, pp. 4105-4115.

[10] A. Angert, C.D. Cappa and D. DePaolo, "Kinetic 17O effects in the hydrologic cycle: Indirect evidence and implications" Geochimica et Cosmochimica Acta, 68, 2004, pp. 3487-3495.

[11] J. Jouzel and L. Merlivat, "Deuterium and Oxygen 18 in precipitation: Modelling of the isotopic effects during snow formation", Journal of Geophysical Research, 89, 1984, pp. 11749-11757.

[12] J.R. Petit, J.W.C. White, N.W. Young, J. Jouzel and Y.S. Korotkevich, "Deuterium Excess in Recent Antarctic Snow", Journal of Geophysical Research, 96, 1991, pp. 5113-5122.

[13] P. Ciais and J. Jouzel, "Deuterium and oxygen 18 in precipitation: Isotopic model, including mixed cloud processes", Journal of Geophysical Research, 99, 1994, pp. 16793 - 16803.

[14] S. Joussaume, R. Sadourny and J. Jouzel, "A general circulation model of water isotope cycles in the atmosphere", Nature, 311, 1994, pp. 24-29.

[15] J. Jouzel, G.L. Russell, R.J. Suozzo, D. Koster, J.W.C. White and W.S. Broecker, "Simulations of the HDO and $H_2^{18}O$ atmospheric cycles using the NASA GISS general circulation model: The seasonal cycle for present-day conditions", J. Geophys. Res., 92, 1987, pp. 14739-14760.

[16] G. Hoffmann, M. Werner, and M. Heimann, "The Water Isotope Module of the ECHAM Atmospheric General Circulation Model - A study on Time Scales from Days to Several Years", J. Geophys. Res., 103, 1998, pp. 16,871-16,896.

[17] H. Craig, "Isotopic variations in meteoric waters", Science, 133, 1961, pp. 1702.

[18] IAEA, "GNIP Maps and Animations", International Atomic Energy Agency, Vienna, 2001, Accessible at *http://isohis.iaea.org*.

[19] V. Masson-Delmotte, H. Shugui, A. Ekaykin, J. Jouzel, A. Aristarain, R.T. Bernardo, D. Bromwhich, O. Cattani, M. Delmotte, S. Falourd, M. Frezzotti, H. Gallée, L. Genoni, A. Landais, M. Helsen, G. Hoffmann, J. Lopez, V. Morgan, H. Motoyama, D. Noone, H. Oerter, J.R. Petit, A. Royer, R. Uemura, G. Schmidt, E. Schosser, J. Simões, E. Steig, B. Stenni, M. Stievenard, F. Vimeux and J.W.C. White, "A review of Antarctic surface snow isotopic composition: observations, atmospheric circulation and isotopic modeling", Journal of Climate 21, 2008, pp. 3359-3387.

[20] W. Dansgaard, "Stable Isotopes in Precipitation" Tellus, 16, 1964, pp. 436-468.

[21] A. Angert, S. Rachmilevitch, E. Barkan and B. Luz, "Effect of photorespiration, the cytochrome pathway, and the alternative pathway on the triple isotopic composition of atmospheric O_2", Global Biogeochemical Cycles 17, 2003, doi:10.1029/2002GB001933.

[22] A. Landais, E. Barkan and B. Luz "The record of $\delta^{18}O$ and ^{17}O-excess in ice from Vostok Antarctica during the last 150,000 years", Geophys. Res. Let, 35, 2008, doi:10.1029/2007GL032096.

[23] H.A.J. Meijer and W.J. Li, "The use of electrolysis for accurate $\delta^{17}O$ and $\delta^{18}O$ isotope measurements in water", Isotopes Environ. Health Stud., 34, 1998, pp. 349-369.

[24] M. Frezzotti, M. Pourchet, O. Flora, S. Gandolfi, M. Gay, S. Urbini, C.Vincent, S. Becagli, R. Gragnani, M. Proposito, M. Severi, R. Traversi, R. Udisti and M. Fily, "Spatial and temporal variability of snow accumulation in East Antarctica from traverse data", Journal of Glaciology, 51, 2005, pp. 113-124.

[25] M. Majoube, "Fractionnement en oxygène-18 et en deutérium entre l'eau et sa vapeur", J. Chem. Phys., 58, 1971, pp. 1423-1436.

[26] W.A. Van Hook, "Vapor pressures of the isotopic waters and ices." J. Phys. Chem., 72, 1968, pp. 1234-1244.

[27] L. Merlivat and G. Nief, "Fractionnement isotopique lors des changements d'état solide-vapeur et liquide-vapeur de l'eau à des températures inférieures à 0°C", Tellus 19, 1967, pp. 122-127.

[28] M. Majoube, « Fractionnement en oxygène 18 entre la glace et la vapeur d'eau. », J Climate Phys, 68, 1971, pp. 625−636.

[29] L. Merlivat, "Molecular diffusivities of $H_2^{16}O$, $HD^{16}O$ and $HD^{18}O$ in gases", J. Chem. Phys., 69, 1978, pp. 2864-2871.

[30] C. Lorius, L. Merlivat, and R. Hagemann, "Variation in the Mean Deuterium Content of Precipitations in Antarctica", Journal of Geophysical Research 74, 1969, pp. 7027-7031.

[31] A. Ekaykin, V.Y. Lipenkov , N.I. Barkov, J.R. Petit , and V. Masson-Delmotte, "Spatial and temporal variability in isotope composition of recent snow in the vicinity of Vostok Station: implications for ice-core record interpretation" Annals of Glaciology, 35, 2002, pp. 181-186.

[32] T.A. Neumann and E. D. Waddington, Effects of firn ventilation on isotopic exchange, Journal of Glaciology, 169, 2004, pp. 183-194.

[33] J. Jouzel, C. Lorius, J. R. Petit, C. Genthon, N. I. Barkov, V. M. Kotlyakov and V. M. Petrov, "Vostok ice core: a continuous isotope temperature record over the last climatic cycle (160,000 years)", Nature, 329, 1987, pp. 402-408.

[34] H. Craig and L. Gordon, "Deuterium and oxygen-18 in the ocean and the marine atmosphere" In: E. Tongiorgi (Editor), Stable Isotopes in Oceanographic Studies and Paleotemperatures, Spoleto, 1965, pp. 9-130.

[35] W.A. Brutsaert, "Theory for local evaporation (or heat transfer) from rough and smooth surfaces at ground level", Water Resourc. Res., 11, 1975, pp. 534-550.

[36] W.A. Brutsaert, "The roughness length for water vapor, sensible heat and other scalars", J. Atmos. Sci., 32, 1975, pp. 2028-2031.

[37] L. Merlivat and J. Jouzel, "Global climatic interpretation of the deuterium-oxygen 18 relationship for precipitation", J. of Geophys. Res., 84, 1979, pp. 5029-5033.

[38] S.J. Johnsen, W. Dansgaard and J.W. White, "The origin of Arctic precipitation under present and glacial conditions", Tellus, 41 (B), 1989, pp. 452-469.

[39] J. Jouzel and R.D. Koster, "A reconsideration of the initial conditions used for stable water isotope models", Journal of Geophysical Research, 101, 1996, pp. 22933-22938.

[40] C.D. Charles, D. Rind, J. Jouzel, R.D. Koster, and R.G. Fairbanks, "Glacial-interglacial changes in moisture sources for Greenland: Influence on the ice core record of climate", Science, 263, 1994, pp. 508-511.

[41] M. Werner, M. Heimann and G. Hoffmann, "Isotopic composition and origin of polar precipitation in present and glacial climate simulations", Tellus, 53B, 2001, pp.53-71.

[42] H. Craig and Y. Horibe, "Isotope characteristics of marine and continental water vapour", Trans. Am. Geophys. Union 48, 1967, pp. 135–136.

[43] H. Jacob and C. Sonntag, "An 8-year record of the seasonal variation of 2 H and 18 O in atmospheric water vapour and precipitation at Heidelberg, Germany", Tellus, 43B, 1991, pp. 291–300.

[44] K. Rozanski, C. Sonntag and K.O. Munnich, "Factors controlling stable isotope composition of European precipitation", Tellus, 34, 1982, pp. 142-150.

[45] W.G. Mook, "Environmental Isotopes in the Hydrological Cycle-Principles and Applications.Volume 1: Introduction-Theory, Methods, Review", UNESCO/IAEA Series, 2002.

[46] J. Worden, D. Noone, K. Bowman and the Tropospheric Emission Spectrometer science team and data contributors, "Importance of rain evaporation and continental convection in the tropical water cycle", Science, 445, 2007, pp. 529-532.

[47] J.R. Lawrence, S.D. Gedzelman, D. Dexheimer, H.-K. Cho, G.D. Carrie, R. Gasparini, C.R. Anderson, K.P. Bowman and M.I. Biggerstaff, "Stable isotopic composition of water vapor in the tropics", J. Geophys.Res.Atmos., 109, 2004, doi:10.1029/2003JD004046.

[48] C. Cappa, M.B. Hendricks, D.J. DePaolo and R.C. Cohen "Isotopic fractionation of water during evapotranspiration". J. Geophys. Res., 108(D16), 2003, doi: 10.1029/2003JD003597.

[49] V. Masson-Delmotte, et al., "Common millenial scale variability of Antarctic and southern ocean temperatures during the past 5000 years reconstructed from EPICA Dome C ice core", The Holocene, 14, 2004, pp. 145-151.

[50] J.L. Kavanaugh and K. M. Cuffey, "Space and time variation of d18O and dD in Antarctic precipitation revisited" Gobal Biogeochemical cycles, 17, 1017, 2003, doi:1010.1029/2002GB001910.

[51] M.R. Helsen, S.W. van de Wal, M.R. van den Broeke, V. Masson-Delmotte, H.A.J. Meijer, M.P. Scheele and M. Werner, "Modelling the isotopic composition of Antarctic snow using backward trajectories: simulation of snow pit records", J. Geophys. Res., 111, 2006, doi: 10.1029/2005JD006524.

[52] G. Delaygue, V. Masson, J. Jouzel, R. Koster and R. Healy, "The origin of Antarctic precipitation: a modelling approach", Tellus, 52 B, 2000, pp. 19-36.

[53] J.R. Gat, W.G. Mook and H.J.R. Meijer ," Stable isotope processes in the water cycle" *Environmental isotopes in the hydrological cycle:* Mook W.G. (ed.). 2 (3), 2000, UNESCO, IAEA: Paris., http://www.iaea.org/programmes/ripc/ih/volumes/vol_two/ChT_II_03.pdf.

[54] J. Jouzel, F. Vimeux, N. Caillon, G. Delaygue, G. Hoffmann, V. Masson-Delmotte and F. Parrenin, "Magnitude of isotope/temperature scaling for interpretation of central Antarctic ice cores", J. Geophys. Res., 108, 2003, doi:10.1029/2002JD002677.

[55] F. Vimeux, K. M. Cuffey and J. Jouzel, "New insights into Southern Hemisphere temperature changes from Vostok ice cores using deuterium excess correction", Earth and Planetary Science Letters, 203, 2002, pp. 829-843.

[56] F. Vimeux, V. Masson, G. Delaygue, J. Jouzel, J-R. Petit and M. Stievenard, “a 420,000 years deuterium excess record from East Antarctica: Information of past changes in the origin of precipitation at Vostok”, J. Geophys. Research, 106 (D23), 2001, pp. 31,863-31,873.